

A Spatially-Resolved X-ray Spectroscopic Analysis of the Luminous Northeastern Rim of the Galactic Supernova Remnant W28 (G6.4-0.1)

*Sarah Norris, Dr. Thomas Pannuti, Mentor, Department of Earth and Space Sciences, College of Science

We present a spatially-resolved spectroscopic analysis of the X-ray luminous northeastern rim of the Galactic supernova remnant (SNR) W28 (G6.4-0.1) using a pointed 50 kilo-second observation made with the Chandra X-ray Observatory. This SNR is well-known for its strong interaction with adjacent molecular clouds located along its northern and eastern borders, as indicated by the detection of hydroxyl (OH) masers. The northeastern rim of W28 is an intriguing morphological feature of the SNR: a large concentration of OH masers have been detected just east of this rim and the spatial distribution of these masers mirrors the morphology of the rim in a striking manner. We have divided the rim into twelve different regions and conducted spectroscopic analysis of each region to search for spatial variations in the rim's X-ray emission. The spectra were all fit simultaneously and successfully with the VAPEC model, which assumes that the X-ray emitting plasma is in collisional ionization equilibrium. The mean fitted temperature of the regions and the fitted elemental abundances of neon, magnesium and iron indicate that the X-ray emission is dominated by swept-up material. We also investigate the physical conditions that facilitate the creation of the high concentration of detected OH masers.

THE GALACTIC SNR W28 (G6.4-0.1) AND ITS REMARKABLE NORTHEASTERN RIM

- Distance: $d \sim 2$ kpc (based on HI observations, CO observations of associated molecular clouds and optical expansion measurements)
- Shell-like radio source ~ 48 arcmin in diameter brightened along the northern and eastern rims -- integrated flux density of ~ 310 Jy at 1 GHz (Dubner et al. 2000, AJ, 120, 1933)
- Centrally-concentrated X-ray source with thermal emission -- northeastern rim only feature clearly detected in X-ray and radio (Rho & Borkowski, 2002, ApJ, 575, 201; Pannuti et al. 2017, ApJ, submitted) -- See Figure 1
- W28 is archetypical MMSNR (Rho & Petre 1998, ApJ, 503, L167) -- do contrasting X-ray and radio morphologies originate from interaction with adjacent molecular clouds?
- Northeastern rim features high concentration of OH masers -- signposts of interaction between W28 and adjacent molecular clouds (Claussen et al. 1999, ApJ, 522, 349) -- See Figure 1
- High X-ray ionization rates of molecular clouds are conducive to the formation of columns of warm OH associated with the formation of OH masers (Wardle 1999, ApJ, 525, L101)

CHANDRA OBSERVATION, DATA REDUCTION AND ANALYSIS

- A pointed observation of the northeastern rim of W28 was conducted with the ACIS-S array aboard *Chandra* on 23 October 2015. The dataset was reduced using standard tools in the CIAO Software Package Version 4.8 (CALDB Version 4.7.2), specifically the CIAO tool *chandra_repro*. Periods of flaring activity were manually flagged to generate good-time-intervals (GTIs). The effective exposure time of the observation after processing was ~ 50 ksec.
- Spectral extraction was accomplished using the CIAO tool *specextract* to generate spectral files for each of the twelve source regions and two background regions (with a minimum binning of 25 counts per bin) along with ancillary response files (ARFs) and redistribution matrix files (RMFs). Spectral fitting was performed using XSPEC Version 12.8.0q (Arnaud 1996, Astronomical Data Analysis Software and Systems V, 101, 17).

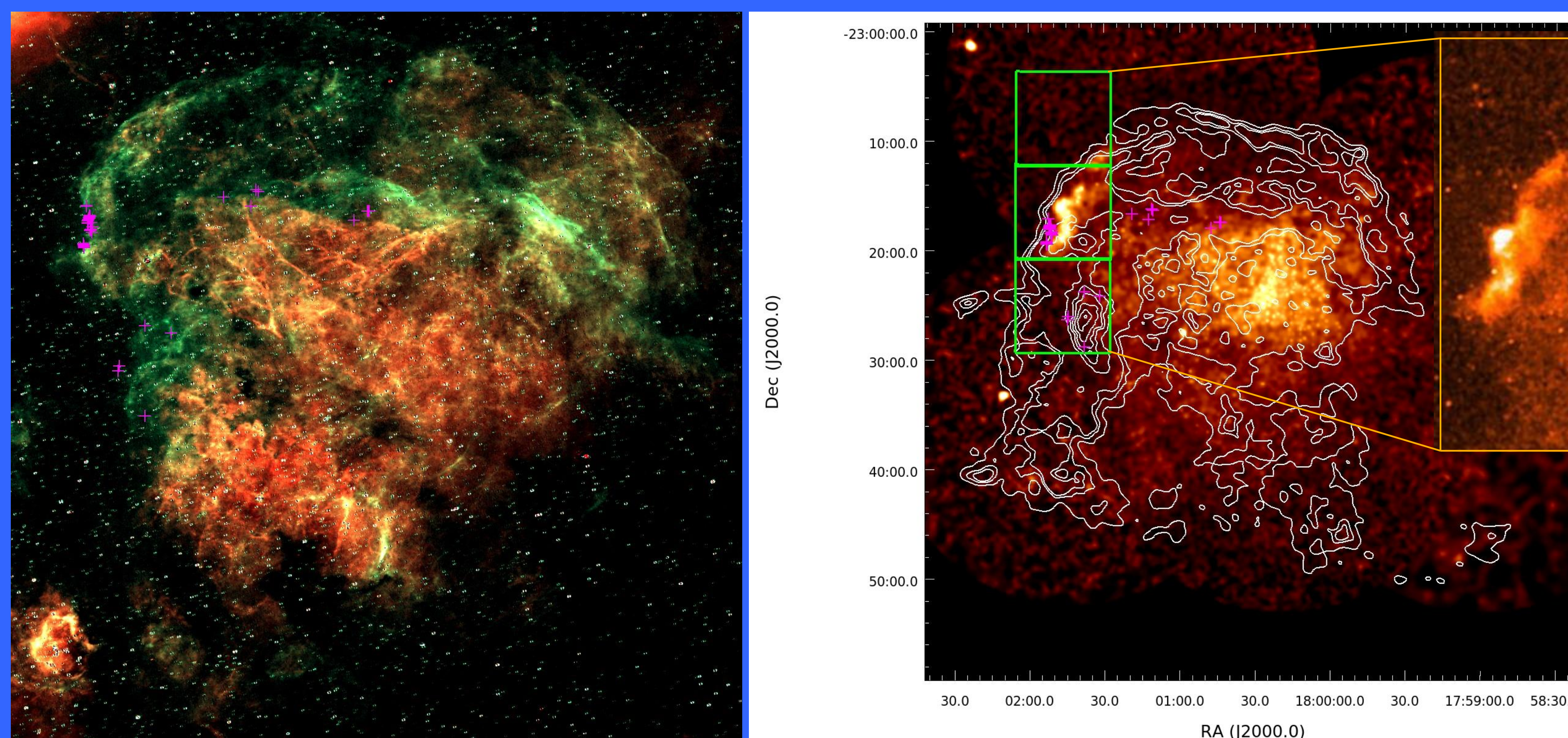
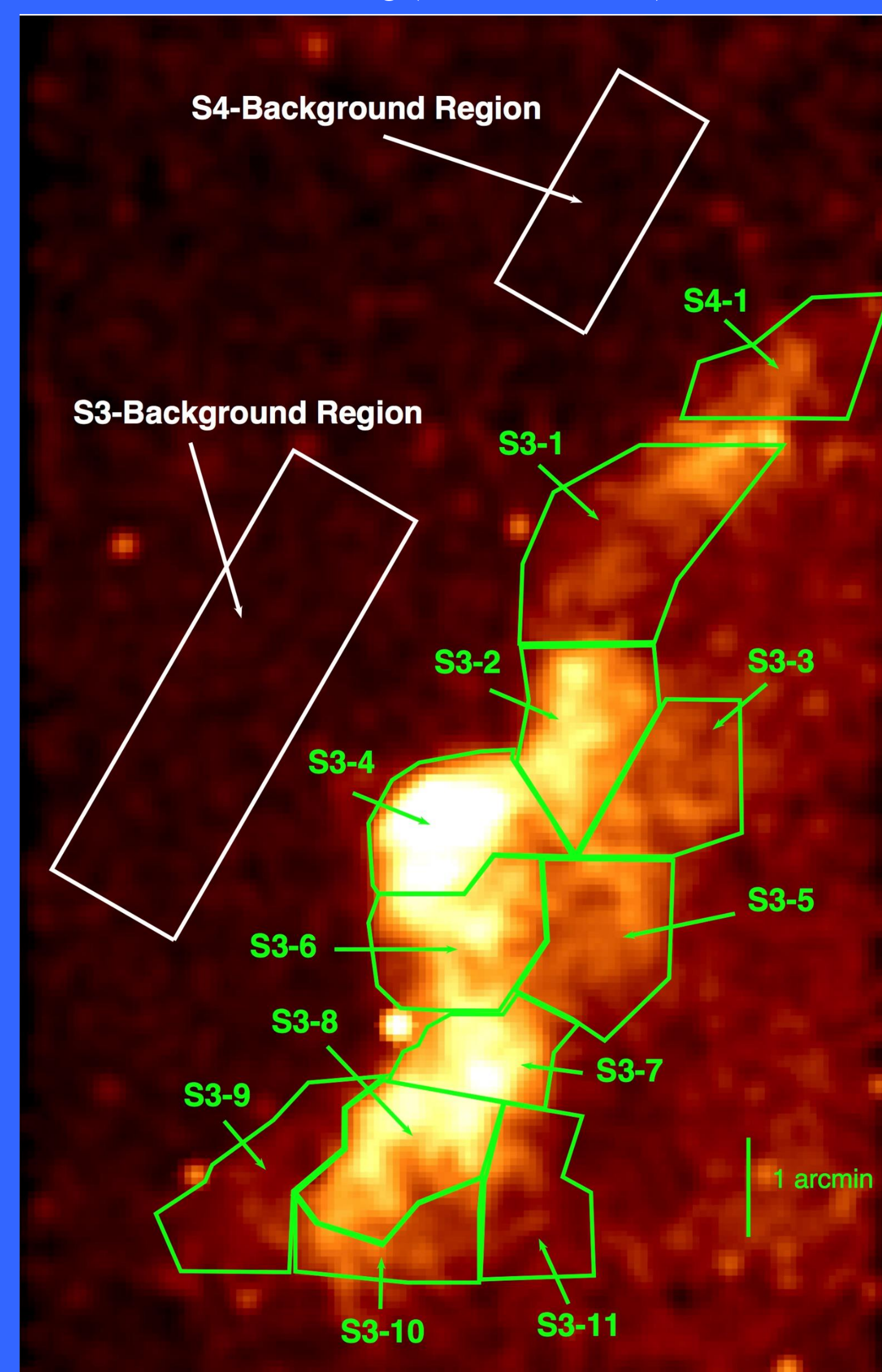


Figure 1 -- (Upper Left). Optical (CTIO) narrow-band image of W28 with H α emission shown in red and [SII] emission shown in green. The locations of known OH masers (Claussen et al. 1999, ApJ, 522, 349) are shown in magenta. Notice the spatial coincidence between the locations of the masers and enhanced [SII] emission along the northern and eastern rims: W28 is believed to be interacting most strongly with molecular clouds at these locations. From Pannuti et al. 2017, ApJ, submitted. (Upper Right) ROSAT HRI mosaicked image of W28. The white contours correspond to radio emission detected by the VLA at a frequency of 1415 MHz (Dubner et al. 2000, AJ, 120, 1933): the contour levels are 0.0035, 0.0075, 0.01, 0.023, 0.03, 0.035, 0.041, 0.0475, 0.05375 and 0.06 Jy/beam. Notice the centrally-concentrated emission along with the bright northeastern rim: this rim is also detected readily in the radio as well. The locations of known OH masers are shown in magenta and the footprints of the ACIS-S2, -S3 and -S4 chips are shown in green. (Upper Right - Inset) An exposure-corrected broadband (0.5 - 7.0 keV) image of the northeastern rim revealing (for the first time) fine structure in the X-ray emission from the rim.



RESULTS - IMAGING

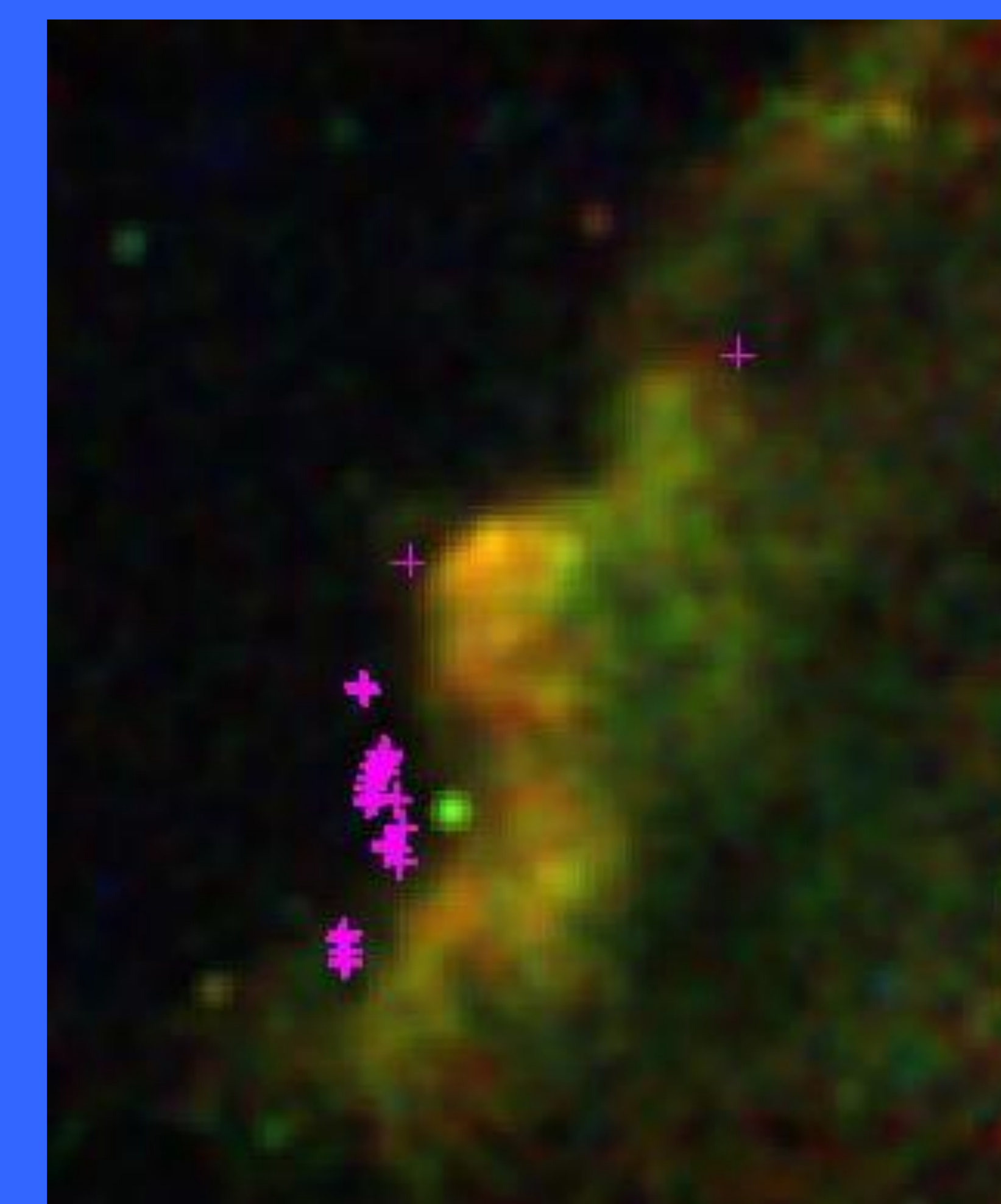


Figure 2 -- Three-color exposure-corrected image of the northeastern rim. Soft (0.5 - 1.0 keV), Medium (1.0 - 2.0 keV) and Hard (2.0-7.0 keV) emission shown in red, green and blue, respectively. Notice the offset with the locations of the known OH masers.

Figure 3 -- (Far Left) Regions of spectral extraction for the ACIS-S3 and ACIS-S4 chips. Regions of background spectrum extraction for the two chips are also included. (Center Left) The extracted spectrum of region S3-4 of the northeastern rim of W28 shown in black. The parameters of the fit are given in Table 1.

Table 1 Spectral Fit to 12 Regions of the Northeast Rim of W28 Using TBABSxVAPEC Model. The regions are listed in order of decreasing declination and from north to south along the northeastern rim. All of the spectra were fitted over the energy range 0.6 keV to 4.0 keV. All quoted error bounds correspond to 90% confidence intervals.

Region	Area (arcsec ²)	kT (keV)	Normalization (cm ⁻⁵)	Electron Number Density n _e (cm ⁻³)
S4-1	5670	0.37 ^{+0.05} _{-0.03}	2.12 x 10 ⁻³	2.98
S3-1	11697	0.31 ± 0.02	5.57 x 10 ⁻³	3.37
S3-2	6708	0.36 ^{+0.02} _{-0.01}	5.23 x 10 ⁻³	4.31
S3-3	6119	0.37 ± 0.02	2.75 x 10 ⁻³	3.27
S3-4	7203	0.31 ^{+0.02} _{-0.01}	1.06 x 10 ⁻³	5.92
S3-5	7544	0.46 ^{+0.03} _{-0.02}	2.01 x 10 ⁻³	2.52
S3-6	7265	0.30 ± 0.01	8.52 x 10 ⁻³	5.29
S3-7	4369	0.31 ^{+0.02} _{-0.01}	5.39 x 10 ⁻³	5.42
S3-8	7095	0.37 ^{+0.02} _{-0.01}	7.99 x 10 ⁻³	5.18
S3-9	6817	0.31 ± 0.04	1.52 x 10 ⁻³	2.30
S3-10	4260	0.33 ± 0.03	2.06 x 10 ⁻³	3.39
S3-11	5066	0.39 ^{+0.04} _{-0.03}	1.35 x 10 ⁻³	2.52

CONCLUSION

For the joint fit to all of the spectra, $\Delta\chi^2 = \chi^2 / \text{degrees of freedom} = 888.85 / 803 = 1.11$. The column density was tied together with a fitted value of $N_{\text{H}} = 1.05 \pm 0.04 \times 10^{22} \text{ cm}^{-2}$ for all 12 regions for this joint fit. The elemental abundances of neon, magnesium and iron were also tied together for all 12 regions for this joint fit, with values of $\text{Ne} = 0.60^{+0.05}_{-0.04}$, $\text{Mg} = 0.69^{+0.06}_{-0.05}$ and $\text{Fe} = 0.48^{+0.06}_{-0.05}$ (measured relative to solar). The abundances of all other elements were frozen to solar values. The mean fitted temperature of the regions and the fitted elemental abundances of neon, magnesium and iron indicate that the X-ray emission is dominated by swept-up material.